Title

PMR5, an acetylation protein at the intersection of pectin biosynthesis and defense against fungal pathogens

Journal

The Plant Journal, 100(5)

ISSN

0960-7412

Authors

Chiniquy, Dawn

Underwood, William

Corwin, Jason

et al.

Publication Date

2019-12-01

DOI

10.1111/tpj.14497

Peer reviewed

PMR5, an acetylation protein at the intersection of pectin biosynthesis and defense against fungal pathogens

Dawn Chiniquy[1,2,*,†], William Underwood[1,2,‡], Jason Corwin[3,§], Andrew Ryan[1,2], Heidi Szemenyei[1,2], Candice C. Lim[1,2], Solomon H. Stonebloom[4], Devon S. Birdseye[4], John Vogel[1,5], Daniel Kliebenstein[3], Henrik V. Scheller[1,4,6] and Shauna Somerville[1,2]

[1]*Department of Plant and Microbial Biology, University of California, Berkeley, CA, 94720, USA,*
[2]*Energy Biosciences Institute, Berkeley, CA, 94720, USA,*
[3]*Department of Plant Sciences, University of California, Davis, CA, 95616, USA,*
[4]*Joint BioEnergy Institute, Emeryville, CA, 94608, USA,*
[5]*Joint Genome Institute, Walnut Creek, CA, 94598, USA, and*
[6]*Environmental Genomics and Systems Biology Division, Lawrence Berkeley National Laboratory, Berkeley, CA, 94720, USA*

ABSTRACT

Powdery mildew (*Golovinomyces cichoracearum*), one of the most prolific obligate biotrophic fungal pathogens worldwide, infects its host by penetrating the plant cell wall without activating the plant's innate immune system. The Arabidopsis mutant *powdery mildew resistant 5* (*pmr5*) carries a mutation in a puta-tive pectin acetyltransferase gene that confers enhanced resistance to powdery mildew. Here, we show that heterologously expressed PMR5 protein transfers acetyl groups from [^{14}C]-acetyl-CoA to oligogalactur-onides. Through site-directed mutagenesis, we show that three amino acids within a highly conserved esterase domain in putative PMR5 orthologs are necessary for PMR5 function. A suppressor screen of muta-genized *pmr5* seed selecting for increased powdery mildew susceptibility identified two previously charac-terized genes affecting the acetylation of plant cell wall polysaccharides, *RWA2* and *TBR*. The *rwa2* and *tbr* mutants also suppress powdery mildew disease resistance in *pmr6*, a mutant defective in a putative pectate lyase gene. Cell wall analysis of *pmr5* and *pmr6*, and their *rwa2* and *tbr* suppressor mutants, demonstrates minor shifts in cellulose and pectin composition. In direct contrast to their increased powdery mildew resis-tance, both *pmr5* and *pmr6* plants are highly susceptibile to multiple strains of the generalist necrotroph *Botrytis cinerea*, and have decreased camalexin production upon infection with *B. cinerea*. These results illustrate that cell wall composition is intimately connected to fungal disease resistance and outline a poten-tial route for engineering powdery mildew resistance into susceptible crop species.

INTRODUCTION

Plant cell walls are a dynamic terrain, undergoing frequent construction and deconstruction to meet the needs of the developing plant (Somerville *et al.*, 2004; Keegstra, 2010). Cell walls must be malleable for growth, sturdy for water transport, flexible to allow movement without breakage and remain able to be deconstructed at precisely timed ripening stages (Cosgrove, 2005). Modifications of specific cell wall polysaccharides, including acetylation and methylation, allow for this plasticity during growth and development, providing flexibility during growth and strength when growth is complete. Pectins, a diverse group of cell wall polysaccharides rich in galacturonic acid residues, are often acetylated or methylated to various degrees, a process that prevents the formation of calcium-mediated interactions, which makes the cell wall more expandable (Liners *et al.*, 1992; Harholt *et al.*, 2010). Upon pathogen attack, pectin fragments elicit a defense response in plants (Lionetti *et al.*, 2012; Bellincampi *et al.*, 2014), making pectin an essential component of the immunity

detection system (Ferrari *et al.*, 2013). Specifically, oligogalacturonides (OGAs), which are fragments of the homogalacturonan domains of pectin, are released by the cell wall as degradation byproducts following exposure to pathogen endopolygalacturonases and endopectate lyases.

Powdery mildew is a disease caused by biotrophic fungal pathogens that affects over 9000 dicot species and 600 monocot species, including many economically valuable crops; with such a wide host range, it is one of the most prevalent plant pathogens worldwide (Glawe, 2008). To gain access to the host, the powdery mildew fungus uses a combination of pressure and a specialized cocktail of cell wall degrading enzymes that function without triggering the plant's elaborate defense system (Schulze-Lefert and Vogel, 2000). Currently, powdery mildew growth is contained by expensive year-round chemical applications and breeder-developed varietals. Modern engineering approaches have the potential to decrease the environmental impact of fungicides, and pectin modification is an effective target in multiple agricultural systems (Ferrari *et al.*, 2008; Osorio *et al.*, 2011; Volpi *et al.*, 2011; Lionetti *et al.*, 2014); however, we are limited in our understanding of pectin biosynthesis and how this modification would affect resistance to other pathogens. Of the estimated 65 enzyme activities required for the synthesis of the variety of pectic polysaccharides (Mohnen, 2008; Caffall and Mohnen, 2009; Harholt *et al.*, 2010), very few have yet been characterized.

Previously, 20 mutants resistant to the powdery mildews *Golovinomyces cichoracearum* and *Golovinomyces orontii* were identified through an ethyl methanesulfonate (EMS)-generated forward genetics screen in *Arabidopsis thaliana* (Vogel and Somerville, 2000). One of these mutants, *powdery mildew resistant 5* (*pmr5*), is mutated in a gene encoding a member of the trichome birefringence-like (TBL) /DUF231 family of proteins that includes several proteins involved in cell wall biosynthesis and modification. Powdery mildew resistance in *pmr5* does not appear to trigger any known defense signaling pathways, including salicylic acid, jasmonic acid and ethylene defense pathways, which suggests that *pmr5*-mediated resistance may act through a previously uncharacterized defense pathway (Vogel *et al.*, 2004).

Characterized proteins from the TBL/DUF231 family include a diversity of cell wall modifiers: AXY4 (acetylation of xyloglucan) (Gille *et al.*, 2011b; Zhu *et al.*, 2014), TBR (trichome birefringence), a gene involved in cellulose biosynthesis (Bischoff *et al.*, 2010), ESK1 (eskimo 1) involved in the acetylation of xylan (Xin *et al.*, 2007; Yuan *et al.*, 2013; Urbanowicz *et al.*, 2014), TBL3 and TBL31, which are required for the 3-*O*-monoacetylation of xylan (Yuan *et al.*, 2016), and TBL10, which *O*-acetylates rhamnogalacturonan I (Stranne *et al.*, 2018). From another protein family, RWAs (reduced wall acetylation) are likely to function as transporters for acetyl-CoA from the cytosol to the Golgi lumen to provide substrate for acetylation (Manabe *et al.*, 2013), and AXY9 is suggested to produce an acetylated intermediate for the acetylation of xyloglucan (Schultink *et al.*, 2015). Of the four RWA proteins in Arabidopsis, RWA2 is particularly important for pectin acetylation (Manabe *et al.*, 2013). RWAs are also highly homologous to the Cas1p (capsule structure 1) protein from *Cryptococcus neoformans*, which was identified in a *Cas* mutant deficient in acetylation of its coat polysaccharide (Janbon *et al.*, 2001). Interestingly, PMR5 has also been identified as homologous to Cas1p as both have the same esterase domain containing an enzymatic triad within the DUF231 domain (Anantharaman and Aravind, 2010). In the DUF231 family, only PMR5 has been implicated in disease resistance, although the freezing tolerance of *esk1* and the drought tolerance of *TBL10* are both interesting pleiotropic abiotic stress-related traits in this family.

In this study, we demonstrate that PMR5 is a protein involved in the acetylation of pectin capable of adding acetyl groups to galacturonic acid (GalA) oligosaccharides. We show through site-directed mutagenesis that three amino acid residues, previously identified as the DUF231 enzymatic triad, are essential to PMR5 function. Furthermore, we show that putative *PMR5* orthologs in *Hordeum vulgare* (barley), *Oryza sativa* (rice), *Sorghum bicolor* and *Triticum aestivum* (wheat) complement the *pmr5* mutant, illustrating potential routes for engineering resistance. Additionally, through a forward-genetics screen we show that mutations in two previously characterized cell wall synthesis genes, *TBR* and *RWA2*, suppress *pmr5*-mediated resistance to powdery mildew, offering more insight into the connection between pectin acetylation and disease resistance. Finally, we offer evidence that the same cell walls shifts that improve resistance to the biotrophic powdery mildew fungus compromise resistance to the necrotrophic fungus *Botrytis cinerea*, highlighting the importance of considering microbial ecology when engineering resistance.

RESULTS

Cell walls in *pmr5* have altered pectin, decreased acetate and decreased cellulose in 5-week-old leaves

As PMR5 is part of the DUF231 family that contains cell wall-modifying enzymes, we first tested whether there were developmental shifts in cell wall sugar content. We conducted a survey of *pmr5* mutant cell wall monosaccharide content at 7 days post germination (in seedlings), in 3- and 5-week-old leaves, and in young stems (Figure S1). The GalA content in 3-week-old leaves is consistent with the previously reported uronic acid contents of *pmr5* in 18-day-old leaves (Vogel *et al.*, 2004). Notably, the levels of the major backbone sugar of pectins, GalA, were similar across a variety of developmental stages and tissues, with

the exception of 5-week-old leaf tissue, where we observed several shifts in pectic sugars: 17% decrease in GalA, 9% decrease in Rha, 27% increase in Ara and 12% decrease in Gal, relative to the wild type (Figures 1a and S1). In addition, 5-week-old leaves also showed a 12% decrease in cell wall acetyl ester content (Figure 1b) and a 23% decrease in cellulose content (Figure 1c). Sequential extraction of the 5-week-old leaf cell walls indicated the greatest difference in Rha, Ara and Gal contents to be primarily in the sodium carbonate fraction, a fraction rich in the pectic polysaccharide rhamnogalacturonan I (RG-I) (Figure S2) (Brummell, 2006). RG-I is composed of a backbone of alternating GalA and Rha, with arabinan and galactan side chains. Notably, the decrease in GalA was much larger than the decrease in Rha, indicating that not only RG-I but also homogalacturonan was decreased in the mutant, in addition to decreased cellulose and acetyl ester content.

PMR5 adds acetyl residues to pectin fragments using [^{14}C]-acetyl-CoA as an acetyl donor

Based on phylogenetic analysis and cell wall biochemistry, we hypothesized that PMR5 is a pectin acetyltransferase involved in adding acetyl groups to the GalA residues on the homogalacturonan or RG-I chain. Additionally, OGAs (10–15 mer) are known to form calcium bridges and are biologically active in the plant defense response (Ferrari *et al.*, 2013). As OGAs are not commercially available, we used a previously developed method (Ferrari *et al.*, 2007) to degrade PGA into small- (2–10 mer) and medium-sized (10–25 mer) OGAs, purified them for use as substrates in these activity assays, and confirmed their enriched size range by high-performance anion-exchange chromatogra-phy (HPAEC) (Figure S3).

We synthesized *PMR5* cDNA without the transmem-brane domain and purified the protein from *Escherichia coli* cells to use in *in vitro* activity assays. Few other pro-teins appeared present at the final elution step on a Gel-Code™ Blue stained gel, and the band that was detected in high quantities was at ~80 kDa, the size of the pre-dicted MBP-PMR5-Myc-His protein (Figure S4). This band was further confirmed to be MBP-PMR5-Myc-His by mass spectrometry sequencing.

To determine the biochemical activity of the purified PMR5 protein, we incubated freshly purified PMR5 protein with short- and medium-length OGAs and [^{14}C]-acetyl-CoA at varied pH levels. We used a method modified from Rennie *et al.* (2012) to separate the unincorporated [^{14}C]-acetyl-CoA by paper chromatography. Negative controls included both reactions pre-mixed with termination buffer at a range of pH values and reactions lacking the acceptor. The PMR5 protein had similar activity levels with short- and medium-length OGAs at pH 5.0–5.5, whereas significant activity at pH levels of up to 7.0 was only observed with medium-length OGAs (Figure 2). The optimal pH value for

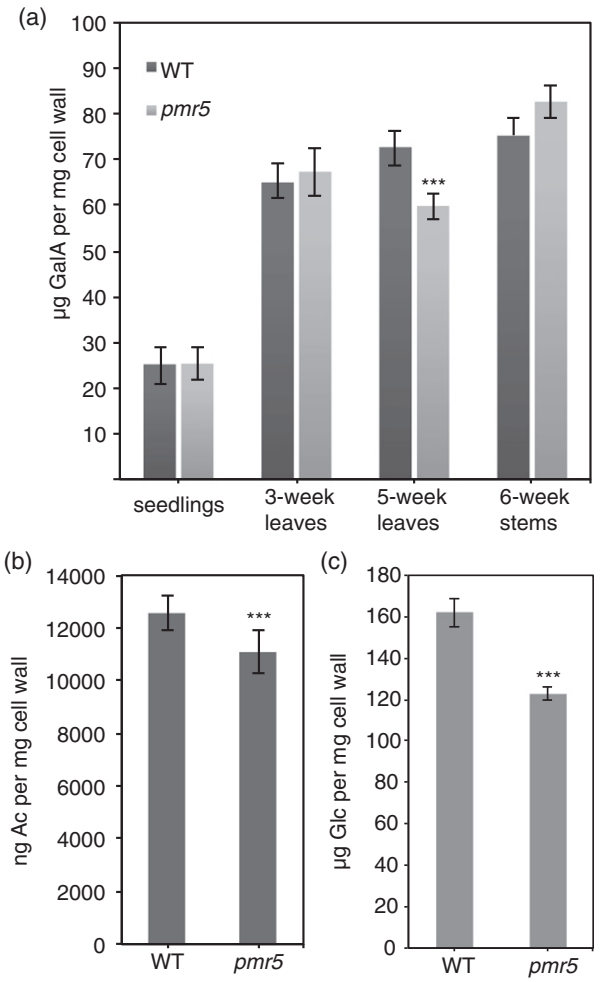

Figure 1. The cell wall biochemistry of the *pmr5* mutant. (a) Shift in cell wall galacturonic acid (GalA) content, indicative of pectin, as the plant grows. Error bars show SDs (n = 3). (b) Decreased total wall-bound acetyl ester content of *pmr5* cell walls in 5-week-old leaves. Error bars represent SEs (n = 8). (c) Cellulose content of 5-week-old leaves. Error bars represent SEs (n = 6). Significantly different from the wild type (WT) by Student's t-test: ***$P < 0.001$.

the medium-length OGAs was consistent with expectations for an endomembrane protein (Golgi, pH 6.2–6.3, endoplasmic reticulum, ER, pH 7–7.5), but we cannot explain the lack of detectable activity with short OGAs at the higher pH values. Determining the optimal substrate was limited by the lack of commercially available OGAs, but we were able to confirm that the PMR5 protein transfers acetic acid esters to the OGAs.

An evolutionarily conserved catalytic triad is necessary for PMR5 function

Based on structural conservation with fungal Cas1p proteins, three amino acids are the enzymatic triad that is essential for the enzymatic acyltransferase function (Anantharaman and Aravind, 2010). We used site-directed

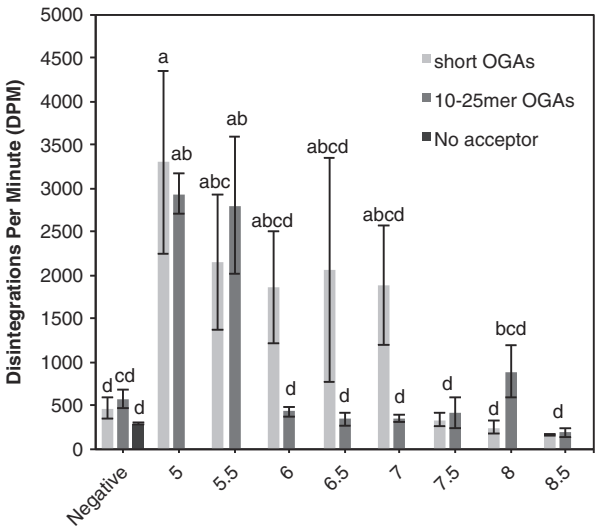

Figure 2. Purified PMR5 protein activity. Purified PMR5 protein expressed without the transmembrane domain in *E. coli* cells shows acetyltransferase activity with [^{14}C]-acetyl-CoA donor and different lengths of oligogalacturonides as acceptors. SE (n = 3). Statistical significance was evaluated with an ANOVA analysis followed by a Tukey's *post hoc* test. Means with the same letter are not significantly different at a P-value of 0.05.

mutagenesis to determine whether these amino acids and the associated enzymatic functions are essential for PMR5 function. To monitor PMR5 expression and localization, we first created a *PMR5*-GFP fusion with the native *PMR5* promoter. The transformation of *pmr5* with *pPMR5::PMR5-GFP* resulted in the complementation of *pmr5* morphological defects and the restoration of powdery mildew susceptibility (Figure 3a). To evaluate putative PMR5 catalytic triad residues, we used site-directed mutagenesis to introduce alanine substitutions at S142, D379 and H382 of the *pPMR5::PMR5-GFP* construct. Upon transformation of *pmr5* with the site-directed mutant constructs the mutant proteins accumulated to similar levels as the wild-type proteins, although the D379A mutant exhibited a somewhat lower level of GFP signal (Figure S9); however, each of the three site-directed mutations (S142A, D379A and H382A) abolished the complementation by the *pPMR5: PMR5-GFP* construct in the *pmr5* mutant background, both in terms of morphological phenotype and powdery mildew resistance (Figure 3a). These observations indicate that the putative catalytic triad amino acids are necessary for PMR5 function.

As indicated by Anantharaman and Aravind (2010), the catalytic triad is well conserved across many phyla (Figure S5). To determine how well conserved PMR5 is across other plant species, using BLAST we found that putative orthologs from barley, rice, sorghum and *Vitis vinfera* (grapevine) were highly conserved at the amino acid level. In all of these four species the catalytic triad was conserved (Figure S6).

To determine whether PMR5 function is conserved in these other species, we cloned the four putative orthologs from barley, rice, sorghum and wheat into a construct driven by the native *PMR5* promoter to determine whether these constructs could complement the *pmr5* mutant. All four constructs complemented the mutant and restored the leaf phenotype and size, as well as restoring powdery mildew disease susceptibility similar to wild type plants (Figure 3b). This suggests that the function of PMR5 is conserved in these four species and that site-directed mutagenesis of one of the three amino acids in the catalytic triad could effectively abolish PMR5 function in these other species. Collectively, these discoveries open the possibility of using CRISPR-Cas9 engineering to improve powdery mildew resistance into a wide variety of crop species plants by targeted swapping and mutation of the *PMR5* gene.

rwa2 and *tbr1* mutants suppress powdery mildew disease resistance in *pmr5* and *pmr6*

To identify additional genes involved in *pmr5*-mediated powdery mildew resistance, we conducted a genetic suppressor screen of *pmr5*. Bulked *pmr5* seeds were EMS mutagenized and the progeny were screened as described by Vogel and Somerville (2000) for the restoration of susceptibility to powdery mildew. Twenty suppressors of *pmr5* were isolated from independent pools of M_2 seeds. Of these 20 suppressors, two mapped to another Cas1p protein family member, At3g06550 (RWA2), and one mapped to a DUF231 family member, At5g06700 (TBR1). Characterized mutant lines for *rwa2* and *tbr1* were crossed with *pmr5* to confirm that these genes were responsible for the suppression of *pmr5* resistance (Figure 4a). Both *RWA2* and *TBR1* are characterized as genes affecting the acetylation of plant cell wall polysaccharides. One other powdery mildew-resistant mutant, *pmr6*, was previously characterized as having reduced esterification of cell wall pectin by Fourier-transform infrared (FTIR) spectroscopy (Vogel *et al.*, 2002). To test whether these two cell wall-related suppressors of *pmr5* resistance also could suppress *pmr6* resistance, *tbr1* and *rwa2* mutations were crossed into a *pmr6* background. We found that *pmr6 rwa2* and *pmr6 tbr1* regained the susceptibility to powdery mildew (Figure S8). We then examined the cell wall composition of all four double mutants (*pmr5 rwa2*, *pmr5 tbr1*, *pmr6 rwa2* and *pmr6 tbr1*) to determine whether there were any changes that could be correlated with the resistance phenotype. Monosaccharide composition was analyzed in 3-week-old leaves, which was a time point that showed few differences between *pmr5* and the wild type in our developmental cell wall survey and was the age of the leaf at the time of all powdery mildew inoculations. The double mutants show shifts in the pectic sugars (generally more galacturonic acid, less galactose and less arabinose than the single mutants), although it is difficult to

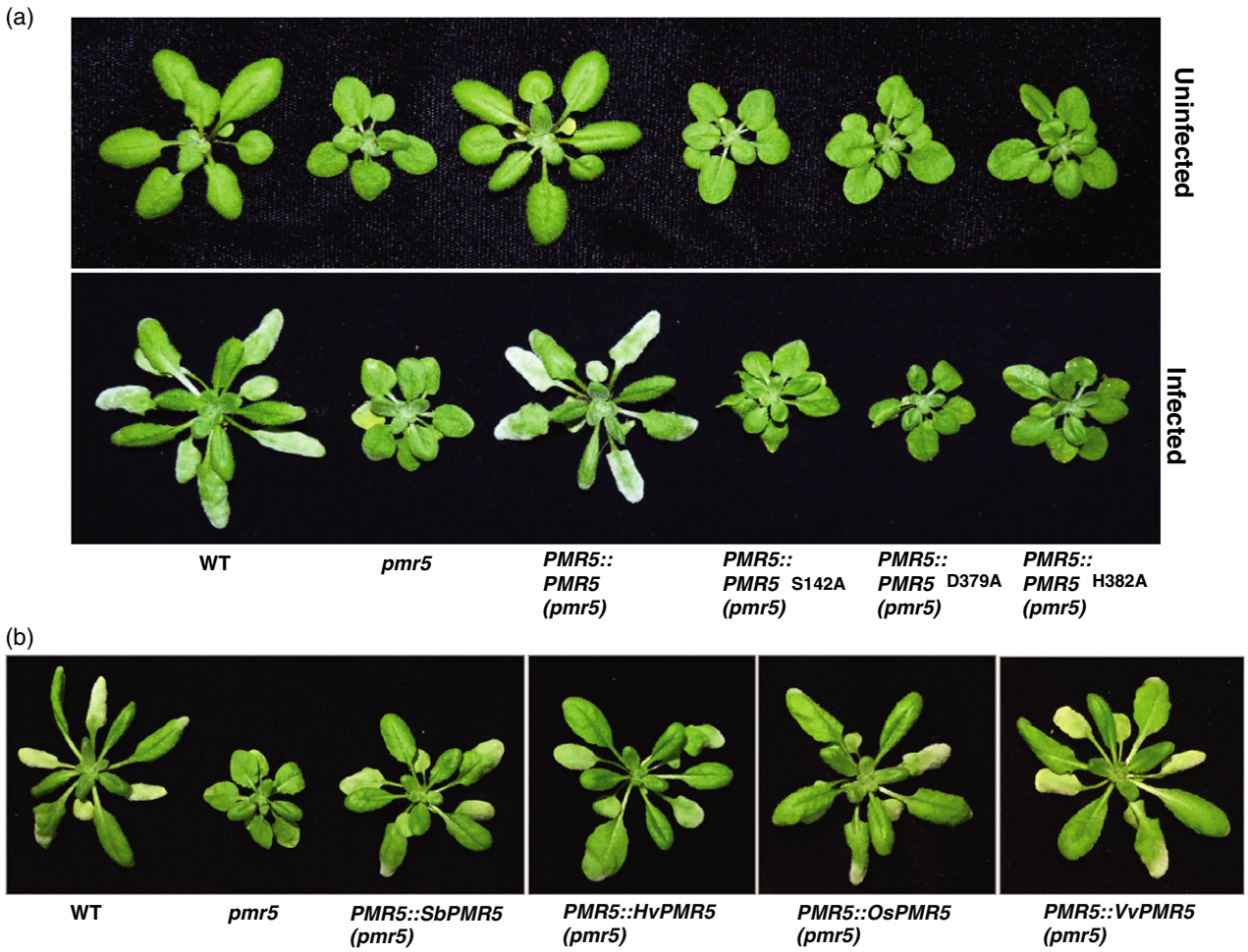

Figure 3. The PMR5 predicted catalytic triad is essential for PMR5 function and may have functional conservation between species. (a) Whole 2 weeks uninfected plant and whole infected plant (10 dpi) show that site-directed amino acid mutants fail to complement *pmr5* in terms of plant size, leaf shape, and disease resistance. (b) Complementation of *pmr5* mutant with four orthologs produces wild type phenotype of leaf size, shape, and powdery mildew disease susceptibility.

determine whether these effects are additive, as the *rwa2* and *tbr1* single mutants also have some shifts relative to the wild type, *pmr5* and *pmr6* plants (Table S1a). Likewise, the cellulose content of these single and double mutants was also decreased, but not in a clearly additive way (Table S1b). This suggests that cellulose content itself is not responsible for resistance in *pmr5* and *pmr6*. The galacturonic acid content of the wild type was closer to *pmr5* and *pmr6* than to their double mutants, and so by itself cannot explain the resistance phenotype, and the other pectic sugar shifts were even less clear to be consistently present in resistant mutants and absent in susceptible ones.

pmr5 resistance is not dependent on oligogalacturonide-mediated defense responses

To determine whether an OGA pre-treatment could improve resistance to *G. cichoracearum*, *pmr5* and the double mutants *pmr5 rwa2* and *pmr5 tbr1* were treated with OGAs of 10–25 mer prior to powdery mildew inoculation, as described by Ferrari *et al.* (2007). The Col-0 wild type had a substantial decrease in the ratio of fungal to plant gDNA, indicating that the OGA pre-treatment does provide temporary protection from *G. cichoracearum* infection (Figure 5b). Additionally, *rwa2* shows high susceptibility to powdery mildew and had the greatest decrease in fungal growth from the OGA pre-treatment. The *pmr5 tbr1* double mutant had slightly less powdery mildew growth with the OGA pre-treatment, and the *pmr5 rwa2* double mutant did not gain any additional protection from powdery mildew infection with the OGA pre-treatment.

Next, we examined two mutants in the OGA defense pathway, *pad3*, a mutant in the enzyme that catalyzes the final step in camalexin biosynthesis, and *wak1*, a wall-associated kinase identified as an intermembrane receptor to extracellular OGAs, and we crossed these two mutations

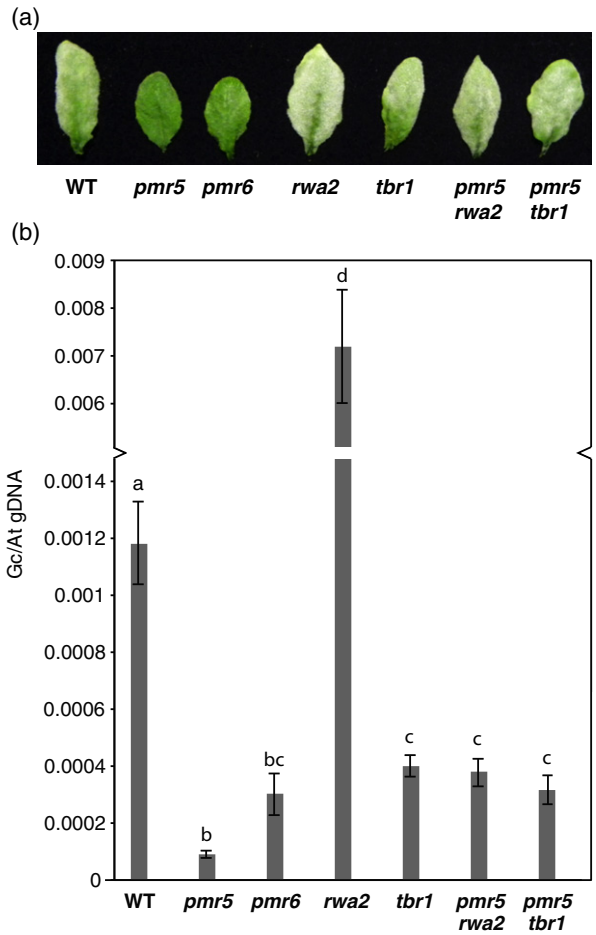

Figure 4. Powdery mildew disease phenotype in double mutants identified through a suppressor screen. (a) Late infection leaf phenotype of double mutants identified through suppressor screen 10 dpi. (b) Early infection phenotype in using the ratio of fungal to plant gDNA 5 dpi in double mutants in the oligogalacturonide defense pathway. Statistical significance was evaluated with an ANOVA analysis followed by a Tukey's *post hoc* test. Means with the same letter are not significantly different at a *P*-value of 0.001. Error bars are SD (n = 12).

into the *pmr5* background (Figure 5a). Fungal spores were measured at 5 days post-inoculation (5 dpi) with *G. cichoracearum* to gain insight into the relative levels of powdery mildew infection (Figure 5c). Much like *rwa2*, *pad3* shows very high susceptibility to powdery mildew. Interestingly, when *pad3* is crossed into *pmr5*, the *pmr5/pad3* double mutant retains powdery mildew resistance. Similarly, *wak1* was highly susceptible to powdery mildew, and this mutation did not suppress the *pmr5*-mediated resistance. Despite the high susceptibility of the *wak1* and *pad3* single mutants, defects in this pathway could not abolish *pmr5*-mediated resistance, indicating that the pathway for which WAK1 and PAD3 detects signals at the cell wall and transmits them through camalexin synthesis is not required for *pmr5*-mediated resistance.

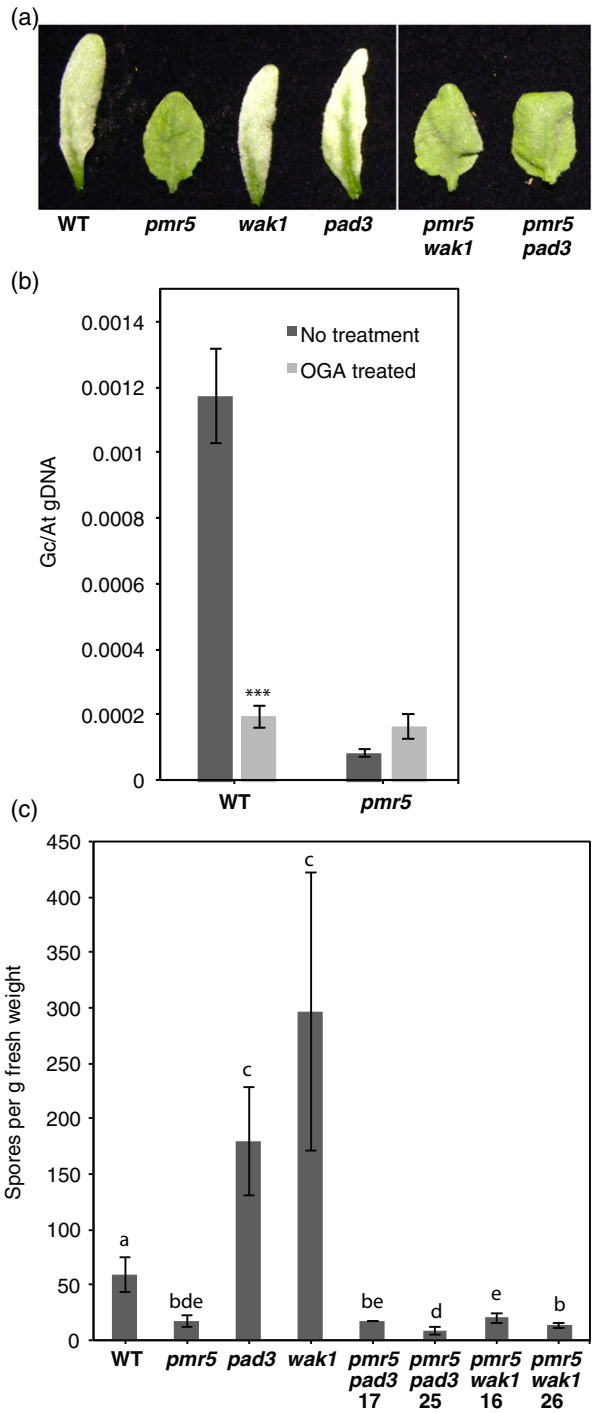

Figure 5. Powdery mildew disease phenotype in single and double mutants connected to oligogalacturonide defense response. (a) Late infection phenotype 10 dpi of powdery mildew, (b) Early infection phenotype with and without an oligogalacturonide (OGA) pre-treatment 24 h before infection (n = 12). The OGA pre-treatment confers resistance to WT but does not enhance resistance in *pmr5*. Statistical significance was evaluated using an ANOVA analysis followed by a Tukey's *post hoc* test. Means with the same letter are not significantly different at a *P* value of 0.05. (c) Early infection phenotype quantified using Gc fungal spore counts 5 dpi in double mutants in oligogalacturonide defense pathway (n = 3). Key: Error bars are SD. Significantly different from WT untreated by *t* test ***$P < 0.001$.

pmr5 and *pmr6* are more susceptible to multiple strains of the necrotrophic pathogen *B. cinerea,* and produce less camalexin upon infection

Biotrophic and necrotrophic pathogens have strikingly different modes of virulence that require different plant innate immune system responses (Glazebrook, 2005); however, the cell wall is typically hypothesized to provide a barrier against both pathogen types, with limited evidence for cell wall resistance mechanisms differentiating between patho-gens. Additionally, the quantitative resistance of the plant to generalist necrotrophic pathogens is dependent on the pathogen genotype (Corwin *et al*., 2016a). To examine if *pmr5*-mediated resistance protects against necrotrophic pathogens, we inoculated *pmr5* and *pmr6* plants, and suppressors of *pmr5*-mediated resistance with four different strains of *B. cinerea* and measured virulence. We also measured camalexin production, a well-established Arabidopsis defense compound against nectrotrophic pathogens. We found that both *pmr5* and *pmr6* mutants had larger lesion areas and produced less camalexin during infection for all isolates of *B. cinerea* relative to the wild type (Figure 6). In contrast to *pmr5* and *pmr6*, the interac-tion of *B. cinerea* with the *rwa2* mutant was highly depen-dent upon the genotype of the pathogen (Manabe *et al*., 2011). Specifically, we found lesion size in *rwa2* to be simi-lar to that in wild type with Apple517 and B05.10 strains, with a non-significant lower lesion size with Supersteak and UKRazz strains (Figure 6a). Similarly, we found elevated camalexin levels in a *rwa2* background only for the UKRazz isolate (Figure 6b). In the *pmr5 rwa2* double mutant, lesion size and camalexin production proved to be largely additive for each isolate, showing an intermediate phenotype between the hyper-susceptible *pmr5* mutant and the hypo-susceptible *rwa2* mutant. Interestingly, *tbr1* and *pmr5 tbr1* were more susceptible to all strains of *B. cinerea* except UKRazz. This may also be explained by the concomitant increase in camalexin content (Figure 6b). Taken together, this suggests that although *pmr5* and *pmr6* are both more resistant to powdery mildew, a biotrophic pathogen, this comes with a trade-off to being more susceptible to *B. cinerea*, a generalist necrotrophic pathogen. Additionally, the lower resistance to *B. cinerea* is correlated with a concomitant decrease in the defense compound camalexin.

DISCUSSION

We report evidence suggesting that PMR5 is a functional acetyltransferase that mediates pectin acetylation on GalA residues, and this leads to altered pathogen resistance. This is evidenced by the observation that the *pmr5* mutant shows decreased acetyl esters extracted from the cell walls in 5-week-old leaves and altered pectic sugar composition, and that the PMR5 protein purified from *E. coli* shows an increased number of OGA products with a radiolabeled acetyl group. PMR5 belongs to the DUF231 protein family that has other members previously characterized to be

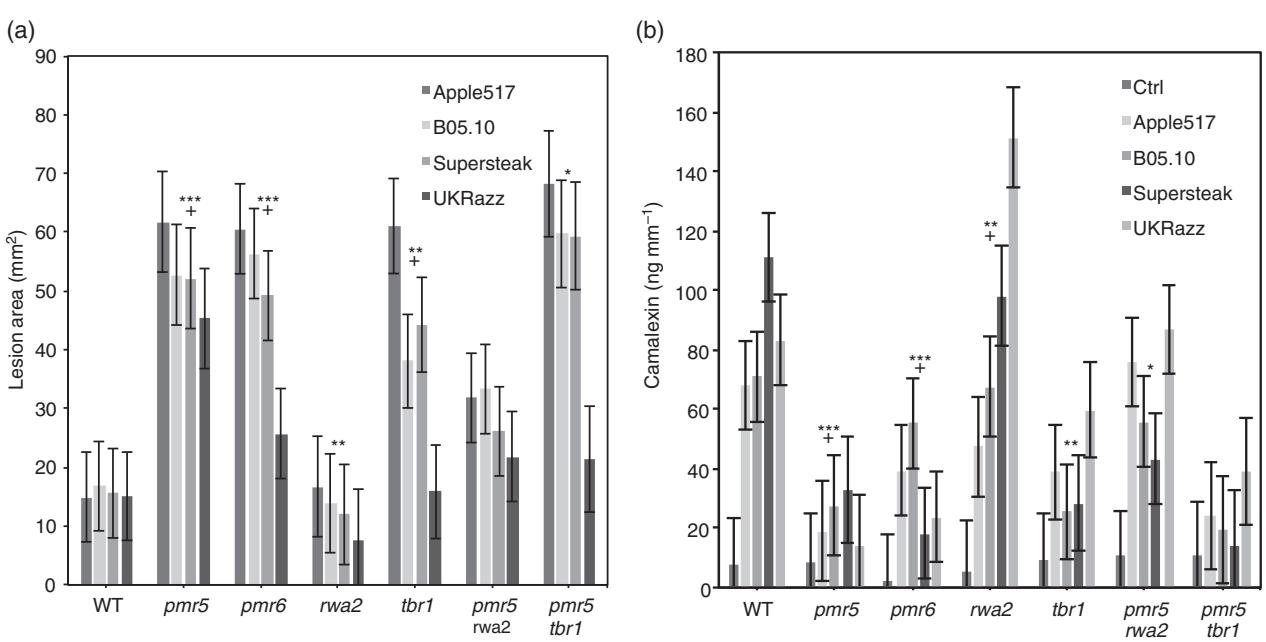

Figure 6. Lesion area and camalexin content of single and double mutants. (a) *pmr5* and *pmr6* are more susceptible to multiple strains of *Botrytis cinerea*. The *pmr5 rwa2* double mutant has an intermediate phenotype of lesion area. SE ($n < 5$). (b) Camalexin leaf content following *B. cinerea* inoculation. Nearly all mutants produce less camalexin than the wild type (WT) control. Camalexin production is inversely proportional to lesion area in most genotypes. SE ($n < 5$). Key: significantly different from WT by ANOVA $*P < 0.05$, $**P < 0.01$, $***P < 0.001$, significantly different among fungal genotypes by ANOVA $+P < 0.05$.

involved in cell wall acetylation. Finally, PMR5 has an esterase domain that is evolutionarily conserved with the *C. neoformans* Cas1p protein (Figure S5) involved in acetylating the fungal coat (Janbon *et al.*, 2001). The acetylation of the fungal coat by Cas1p is essential for the virulence of *Cryptococcus* in animal hosts. The protein is also homologous with the Cas1 mammalian protein involved in the acetylation of sialic acid in certain glycolipids (Arming *et al.*, 2011). This provides important insight into the previously uncharacterized function of PMR5. The activity on OGAs suggests that PMR5 acetylates homogalacturonan domains of pectin, unlike the recently reported TBL10, which is specific for RG-I domains (Stranne *et al.*, 2018). Neither *pmr5* nor *tbl10* is devoid of acetylation of the respective pectin domains, suggesting that additional members of the large TBL family are involved in pectin acetylation. To what extent the acetyltransferases are redundant or acetylate specific subdomains of homogalacturonan and RG-I remains to be determined.

Since the initial characterization of *pmr5* in 2000, the underlying mechanism for powdery mildew resistance in this Arabidopsis mutant has remained a mystery. We hypothesized that *pmr5* powdery mildew resistance resulted from an increase in biologically active OGAs being solubilized by the fungus upon fungal cell wall degradation, leading to the activation of the OGA defense pathway (Ferrari *et al.*, 2013). This hypothesis would be consistent with previous findings that *pmr5*-mediated resistance is not dependent on known resistance pathways (Vogel *et al.*, 2004), as the OGA defense pathway is not dependent on the activation of salicylic acid (SA), jasmonic acid (JA) or ethylene defense pathways (Ferrari *et al.*, 2007). We demonstrated that OGA pre-treatment protected Arabidopsis from *G. cichoracearum* infection in wild-type plants (Figure 5b). One study in wheat found that the wheat powdery mildew (*Blumeria graminis* f. sp. *tritici*) had decreased infection with an OGA pre-treatment that was acetylated as compared with the unacetylated OGAs (Randoux *et al.*, 2010). The defense pathway activated by OGAs requires PAD3, the enzyme that catalyzes the final step in camalexin biosynthesis (Ferrari *et al.*, 2013), and also uses WAK1, a wall-associated kinase that is the receptor for biologically active oligosaccharides that activate this pathway (Brutus *et al.*, 2010; Kohorn and Kohorn, 2012); the *pmr5 pad3* double mutant as well as the *pmr5 wak1* double mutant do not abolish *pmr5*-mediated resistance (Figure 5a,c), indicating that *pmr5*-mediated resistance is not dependent on the activation of the OGA defense pathway, disproving our original hypothesis. Nevertheless, given the high susceptibility of both *wak1* and *rwa2*, and that exogenous application of OGAs decreases powdery mildew infection in the wild type (Figure 5b), it appears that this pathway already provides some baseline defense against powdery mildew.

Although *pmr* mutants are less susceptible to powdery mildew infection, both *pmr5* and *pmr6* mutants are more susceptible to *B. cinerea*. This could be attributed in part to reduced camalexin production following *B. cinerea* inoculation (Figure 6a,b). The *pmr5 tbr1* double mutant and suppressor of *pmr5*-mediated resistance and the *tbr1* single mutant are also more susceptible to *B. cinerea*, with a concomitant lower camalexin production upon infection. Necrotrophs have a larger number of cell wall degrading enzymes than biotrophs (Kämper *et al.*, 2006; O'Connell *et al.*, 2012), and the acetylation of wall polysaccharides affects the association with cellulose and extractability of the cell wall (Selig *et al.*, 2009). It is possible that the relative susceptibility of these mutants to *B. cinerea* results from altered pectic fragments that activate the camalexin synthesis pathway, but it also possible that the altered cellulose content (Figure 6b; Table S1b) makes the cell wall more easily hydrolyzed by the fungus. The B. cinerea fungus may be demolishing the cell walls in the mutant faster, leading to less stress detection (Hamann, 2012) and less camalexin production. This increased stress detection hypothesis would not explain why the *rwa2* mutant increases resistance to just a subset of specific *B. cinerea* strains, however (Manabe *et al.*, 2011) (Figure 6a). This shows that there is significant genetic variation among isolates of *Botrytis* for their virulence in RWA-mediated resistance and PMR5-mediated susceptibility, which could be investigated through genetic mapping in the fungus. Cell wall modifications can lead to defense priming that can alter pathogen penetration and growth (Underwood, 2012). Although *rwa2* has similar monosaccharide and cellulose alterations as the other mutants examined here (Table S1a,b), it is clear that the altered acetylation of cell wall polysaccharides leads to improved resistance through improved stress detection with certain *B. cinerea* strains, although the exact mechanism remains elusive. Indeed, the *rwa2* mutant exhibits a massive induction of defense-related genes in the absence of pathogen infection (Nafisi *et al.*, 2015). Pectin acetylation, as demonstrated for pectin methylesterification, could be a pectin integrity maintenance mechanism that the plant has evolved to render pectin less accessible to the action of hydrolases produced by *Botrytis* strains (Lionetti *et al.*, 2017).

We found that the acetate ester content of *pmr5* leaves was 12% lower than that of the wild type. This is a relatively minor shift to cause such large disease phenotypes as increasing resistance to powdery mildew and decreasing resistance to *B. cinerea*. This illustrates how even slight modifications to cell wall structure lead to trade-offs in fungal disease resistance and highlight the importance of considering microbial ecology when engineering resistance. It also suggests that some plant cell wall composition formulations may have evolved for defense against particular pathogens in environments with that selective pressure,

and some may have evolved for an average level of resistance to commonly found pathogens.

CONCLUSIONS

We show that PMR5 can add acetyl residues to OGAs, and that an exogenously applied OGA treatment to wild-type leaves decreased powdery mildew infection. We show that *pmr5* is more susceptible to *Botrytis* infection and produces less camalexin upon infection, providing more evidence linking the OGA defense pathway to camalexin production; however, two genes essential to this pathway, *wak1* and *pad3* (the final biosynthetic enzyme for camalexin production), when crossed with *pmr5* did not abolish the *pmr5*-mediated resistance, indicating that the camalexin response is not solely responsible for the powdery mildew resistance phenotype. A suppressor screen for the return to susceptibility mapped two of these suppressors to cell wall genes, *RWA2* (*reduced wall acetylation 2*) and *TBR* (*trichome birefringence*), suggesting that *pmr5*-mediated resistance is connected to cell wall structure and/or degradation upon pathogen attack. We found that the three predicted amino acid residues in the catalytic triad are essential for complementing the *pmr5* mutant, and that these amino acids are highly conserved in other species. Putative *PMR5* homologs from barley, grape, rice and sorghum complemented the *pmr5* mutant. The latter two results suggest a future route for engineering resistance.

EXPERIMENTAL PROCEDURES

Plant growth and transformation

Arabidopsis thaliana Heynh. (L) accession Columbia-0 (Col-0) was used for the control line in this study. Arabidopsis seeds were sown on soil (Pro-Mix HP; PRO-MIX, https://www.pthorticulture.com) and stratified for 3 days at 4°C. Plants to be infected with powdery mildew (*G. cichoracearum*, race *UCSC1*) were grown in growth chambers at 22°C with 70% relative humidity (RH) and a 14-h photoperiod. The Arabidopsis mutants used in this study include: *pmr5* (ABRC stock: CS6579), *pmr6-1* (ABRC stock: CS6354), *tbr-1* (ABRC stock: CS3741), *rwa2-3* (SALK_013562), *wak1* (SALK_107175) and *pad3* (SALK_026585C). Homozygous plants were confirmed by polymerase chain reaction (PCR) with gene-specific primers (Table S2). Expression levels of *PMR5* were quantified using qPCR in 3-week-old leaves of the wild type and the *pmr5* mutant, and showed that *PMR5* was expressed ~2.7-fold lower in *pmr5* than in the wild type (Figure S7). Arabidopsis plants were transformed using *Agrobacterium tumefaciens* GV 3101 via the floral-dip method (Clough and Bent, 1998). For selection, seeds were germinated on half-strength MS media with 25 μg ml^{-1} kanamycin. Resistant plants were transferred to soil and grown as described above.

Construction of barley, grape, rice and sorghum *PMR5* ortholog complementation constructs

Sequences for the cDNA for *H. vulgare*, *O. sativa* and *V. vinifera* were synthesized by Life Technologies (ThermoFisher Scientific, https://www.thermofisher.com), as found in the NCBI database (https://www.ncbi.nlm.nih.gov). The *PMR5* gene from *Sorghum bicolor* was obtained by amplification from cDNA extracted from young leaves. Products were sequenced to confirm their identity. Constructs were made using the Gibson assembly technique, with one fragment consisting of the *AtPMR5* upstream promoter region (1000 bp), including the 5′ untranslated region (5′-UTR) and the second fragment consisting of the *PMR5* homolog from each organism, with and without a stop codon. These fragments were introduced into pMDC99 to produce an untagged PMR5 as well as into pMDC107 to produce the GFP-tagged PMR5. Both plasmids were digested with *Pac*I and *Asc*I to produce the vector backbone for assembly. Assembly was performed using a Gibson assembly cloning kit from New England Biolabs (https://www.neb.com).

PMR5 cloning and site-directed mutagenesis

Genomic DNA from Arabidopsis ecotype Col-0 was isolated using a previously described CTAB DNA prep (Lukowitz *et al.*, 1996). To generate the *pPMR5:PMR5-GFP* construct, the genomic region containing the *PMR5* coding sequence and the promoter 1 kb upstream of the coding sequence was amplified from Arabidopsis Col-0 genomic DNA by PCR using the primers listed in Table S2. The amplified product was electrophoresed on a 1% agarose gel, cut from the gel using a razor blade, and purified from the gel slice using a Zymoclean Gel DNA Recovery kit (Zymo Research, https://www.zymoresearch.com), according to the manufacturer's protocol. The *PMR5* product was cloned into a Gateway entry vector using a pCR8/GW/TOPO cloning kit (Life Technologies, ThermoFisher Scientific) according to the manufacturer's protocol. The *pPMR5:PMR5* fragment was subsequently transferred to the vector pMDC107 (Curtis and Grossniklaus, 2003) to fuse GFP in-frame to the C terminus of *PMR5* using LR Clonase (Life Technologies, ThermoFisher Scientific), according to the manufacturer's instructions. Putative esterase catalytic triad mutants PMR5^{S142A}-GFP, PMR5^{D379A}-GFP and PMR5^{H382A}-GFP were generated by site-directed mutagenesis of the *pPMR5:PMR5-GFP* construct described above using a Quikchange II XL site-directed mutagenesis kit (Agilent Technologies, https://www.agilent.com) with mutagenesis primers, according to the manufacturer's protocol (Table S2). For Arabidopsis transformation, all vector constructs were transformed into *Agrobacterium* strain GV3101 (Koncz and Schell, 1986) by electroporation. The cDNA for *SbPMR5* was amplified by PCR using gene-specific primers (Table S2) from first-strand cDNA made from pooled rice samples. Coding sequences for genes were cloned using Gateway technology (Invitrogen, ThermoFisher Scientific) and Gateway-compatible primers (Table S2), as follows: PCR reaction products were gel-purified using the MinElute Gel extraction kit (Qiagen, https://www.qiagen.com) and used for Gibson assembly reactions using the LR clonase enzyme mix (Invitrogen, ThermoFisher Scientific).

Confocal microscopy and image analysis

Plant leaf samples were observed on a confocal microscope system consisting of a Leica DMI 6000 B inverted microscope (Leica Microsystems, https://www.leica-microsystems.com) fitted with a Yokogawa CSU-X1 spinning disk confocal head (Yokogawa Electric Corporation, https://www.yokogawa.com) and a Photometrics QuantEM 512SC EM-CCD camera (Photometrics, https://www.photometrics.com). Microscope control and image acquisition were accomplished using METAMORPH (Molecular Devices, https://www.moleculardevices.com). Pieces were cut from 3-week-old Arabidopsis leaves and mounted in H_2O on microscope slides for imaging. Leaf samples were observed using a 63× water immersion objective. GFP was excited with a 488-nm diode laser and

observed using a 525 ± 25-nm emission filter. Image processing was performed using IMAGEJ (rsbweb.nih.gov/ij/) and PHOTOSHOP (Adobe, https://www.adobe.com). *z*-projections were prepared from 50–150 optical sections (*z*-distance 0.3 μm) by maximum projection using IMAGEJ.

Protein purification from *E. coli* cells

We performed several experiments to test the putative PMR5 pectin acetyltransferase activity. In our initial experiments, we infiltrated *Nicotiana tabacum* (Nicotiana benthamiana) leaves with a vector containing *35S:PMR5-GFP*, confirming expression by microscopy, and isolating the microsomal fraction for an activity assay. We used [^{14}C]-acetyl-CoA as the donor and endogenous substrates as acceptors; however, we were not able to detect a difference in acetyltransferase activity in the PMR5-infiltrated lines above the relatively high level of endogenous acetyltransferase activity.

As a result of this high background acetyltransferase activity, we next established a two-step protein affinity purification system in *E. coli*. The *PMR5* coding sequence was synthesized without the first 29 amino acids (starting at nucleotide 88) with a Myc and His tag at the C-terminal end. Transmembrane domain predictions for PMR5 are from amino acids 6–21, so this effectively deleted the transmembrane domain, making the protein soluble. This was cloned into the pMAL-c2 vector for the pMAL protein fusion and *E. coli* protein purification system, and transformed into Origami B *E. coli* cells (Novagen, now Merck, http://www.merckmillipore.com). A 6-ml starter culture with rich media + glucose (1 L:10 g tryptone, 5 g yeast extract, 5 g NaCl, 2 g glucose, 100 μg ml^{-1} ampicillin) was grown overnight at 37°C, then added to 3 L of rich media + glucose and grown at 37°C to an OD_{600} of 0.5, induced with 0.3 M isopropyl β-D-1-thiogalactopyranoside (IPTG), and grown at 16°C for 16 h before pelleting cells and resuspending them in lysis buffer (50 mM NaH_2PO_4, pH 7.6, 150 mM NaCl, 5% glycerol, 5 mM imidazole, 1 mM 2-mercaptoethanol, 1 EDTA-free Protease Inhibitor Cocktail Tablet; Roche, https://www.roche.com). Cells were lysed using an Avestin E3 Emulsiflex homogenizer and cell debris was pelleted (JA-20 rotor, 48 400 ***g***, 1.5 h, 4°C). Lysate was run through a 10-ml equilibrated column with Ni-NTA resin, washed once with lysis buffer and then eluted with 200 mM imidazole. Flow through was added to an equilibrated amylose resin column, which was washed with a column length of lysis buffer and eluted with lysis buffer + 100 mM maltose. The 80-kDa bands generated from MBP-PMR5-His purification were cut out from a sodium dodecyl sulfate polyacrylamide gel electrophoresis (SDS-PAGE) gel and digested following the UC Berkeley QB3 proteomics/mass spectrometry protocol (http://qb3.berkeley.edu/pmsl/wp-content/uploads/2016/06/In-gel-digestion-protocol.pdf). Briefly, gel fragments were washed with a 100 mM ammonium bicarbonate wash, reduced with 45 mM dithiothreitol (DTT), incubated with 100 mM iodoacetamide for irreversible alkylation, then washed with a 50:50 mix of acetonitrile and ammonium bicarbonate. Gel pieces were dehydrated with acetonitrile and then dried by vacuum centrifuge. Gel pieces were rehydrated with 25 mM ammonium bicarbonate containing modified trypsin (Promega, https://www.promega.com) to digest overnight at room temperature (20–24°C). Peptides were recovered in the supernatant from the overnight digest and then further extracted with 60% acetonitrile/0.1% formic acid and 100% acetonitrile. Samples were analyzed by one-dimensional LC/MS-MS in the UC Berkeley QB3 proteomics/mass spectrometry lab.

Purified protein activity assay

Acetyltransferase activity assays were based on the protocols described by Lee *et al.* (2007) and Rennie *et al.* (2012). Protein was purified as described above, with an added step of concentrating the final protein to 500 μl in a 10 000 molecular weight cut-off (MWCO) Vivaspin concentrator (Viva Products, https://www.vivaproducts.com). Purified protein was quantified on a NanoDrop (NanoDrop 8000 Spectrophotometer, ThermoFisher Scientific), and per reaction, 2 μg protein was added to buffer containing: 50 mM buffer [2-(*N*-morpholino)ethanesulfonic acid (MES) buffer for pH 5.0, 5.5, 6.0 and 6.5 and HEPES buffer for pH 7.0, 7.5 and 8.0], 400 mM sucrose, 5 mM $MnCl_2$, 4 μg oligogalacturonides (10–25 mer), 2 μl (20 nCi μl^{-1}) [^{14}C]-acetyl-CoA (1480 Bq per reaction, specific activity, 40–60 mCi mmol^{-1}; Perkin Elmer, https://www.perkinelmer.com) in a total reaction volume of 50 μl. After incubation at 24°C for 2 h, the reaction was stopped by adding 5 μl of termination buffer [0.3 M acetic acid containing 20 mM ethylene glycol-bis(β-aminoethyl ether)-N,N,N′,N′-tetraacetic acid (EGTA)]. The solution was spotted onto Whatman 3MM chromatography paper (Whatman, now GE Healthcare Life Sciences, https://www.gelifesciences.com), which was then developed for 4 h in 95% EtOH/1 M ammonium acetate, 2:1 (v/v) as the solvent. The radiolabeled oligosaccharides retained at the original spot were cut out and vortexed in 1 ml 100 mM NaOH, then 200 μl 1 M acetic acid to neutralize the NaOH, and then 4 ml of scintillation fluid was added (Ecoscint XR; National Diagnostics, https://www.nationaldiagnostics.com). The level of activity was determined using a scintillation counter set to measure ^{14}C counts for 2 min (Beckman LS 6500; GMI Inc, https://www.gmi-inc.com/). Negative protein controls were heat treated at 100°C for 30 min prior to the addition to reactions. Reactions were set up the same day as protein purification from harvested *E. coli* cells.

Oligogalacturonide (OGA) preparation

The OGAs with a degree of polymerization of 10–25 were prepared by partial hydrolysis of polygalacturonic acid (PGA), based on a protocol described by Bellincampi *et al.* (2000). In a 1-L bottle, 0.4 g PGA (P3889; Sigma-Aldrich, https://www.sigmaaldrich.com) was added to 400 ml of water and brought to a pH of 4.4 using 1 N NaOH. The solution was autoclaved for 45 min, allowed to cool, and brought to a pH of 2 with 1 N HCl, stirring constantly, to precipitate the higher dp OGAs. The solution was then centrifuged at 12 000 ***g*** for 20 min, 363 ml of supernatant was transferred to a 500-ml bottle, and lower dp OGAs (10–25 mers) were precipitated by adding 25 ml 1 M NaOAc and 112 ml 100% ETOH. This solution (pH 6) was placed at 4°C overnight and centrifuged for 30 min at 17 400 ***g***, the supernatant was poured off, and the pellets were resuspended in 50 ml of water, which was dialyzed against 4 L of water for 2 days, changing the water twice. This solution was lyophilized and stored as powder in −20°C. The enrichment of the size ranges of the OGAs in solution (1 mg ml^{-1}) was confirmed by HPAEC on a Dionex ICS3000 CarboPac PA200 system (ThermoFisher Scientific) equipped with a pulsed amperometric detector (PAD), based on Hotchkiss and Hicks (1990) (Figure S3).

Cell wall monosaccharide, acetic acid, and cellulose quantification

For Arabidopsis plants, 3- and 5-week-old leaf tissue as well as 6-week-old stem tissue was collected, frozen in liquid nitrogen and freeze-dried overnight. Alcohol insoluble residue (AIR) preparation and de-starching was performed according to the methods described by Yin *et al.* (2011). For monosaccharide composition analysis, 5 mg was hydrolyzed in 2 M trifluoroacetic acid (TFA) at 120°C for 1 h. The released monosaccharides were separated by HPAEC on a Dionex ICS3000 system equipped with a PAD as described by Harholt *et al.* (2006). For cellulose content analysis,

5 mg of AIR was treated with 72% H_2SO_4 for 1 h at 30°C with shaking and diluted with 715 μl water and autoclaved at 120°C for 1 h. Samples were diluted 200 times with water and run on the HPAEC-PAD system for quantification. All samples were ana-lyzed on a CarboPac PA-20 column (ThermoFisher Scientific) eluted with 2 mm KOH in order to resolve and quantify Fuc, Gal, Glc, Xyl and Man. Samples without concentrated sulfuric acid pre-treatment were further analyzed on a CarboPac PA-20 column eluted with 18 mm of KOH in order to resolve and quantify Rha and Ara. For acetic acid quantification, 10 mg ml^{-1} AIR was saponified by adding an equal volume of 1 M NaOH and incu-bated for 1 h at 26°C with shaking (600 rpm). The de-esterified samples were neutralized with an equal volume of 1 M HCL, pel-leted for 10 min at 20 800 ***g***, and the acetic acid content of the supernatant was determined using the Acetic Acid Kit (K-Acet; Megazyme, https://www.megazyme.com), as described by Gille *et al.* (2011a).

Sequential extraction of cell wall polysaccharides

De-starched AIR (5 mg) was suspended in 0.5 ml 0.05 M CDTA (pH 6.5) for 24 h at room temperature on a thermomixer. The suspension was centrifuged at 48 000 ***g*** at 4°C and the pellet was washed twice with deionized water. The pellet was subsequently sequentially extracted using 0.05 M Na_2CO_3 containing 0.01 M $NaBH_4$ for 24 h at 4°C and washed twice with deionized water. The CDTA and Na_2CO_3 extracts represent the pectin-rich frac-tions. For the hemicellulose-rich fraction, the residual pellet was extracted with 4 M KOH for 24 h at room temperature with shak-ing on a thermomixer. This was centrifuged at 48 000 ***g*** at 4°C to collect the supernatant, which was adjusted to pH 5 with glacial acetic acid and dialyzed against deionized water and lyophilized. Each fraction was then TFA hydrolyzed and run on the HPAEC-PAD system for monosaccharide quantification as described above.

Growth of powdery mildew

Squash, variety Kuta (Park Seed, https://parkseed.com), was used as a host for the production of *G. cichoracearum* UCSC1 inocu-lum. The inoculum was prepared by touching squash plants with infected squash leaves 10–12 days before inoculation. Arabidopsis plants were inoculated at 18–21 days post-germination by placing a 1.3-m settling tower over two flats and tapping between one and three squash leaves over the top of the settling tower. After allowing the spores to settle for 5 min, plants were placed in a high-humidity growth chamber (Adam and Somerville, 1996).

For the OGA pre-treatment of Arabidopsis seedlings, the protocol was based on that described by Ferrari *et al.* (2007). Seedlings (18 day old) grown as described above were treated with OGAs at 24 h and 4 h prior to inoculation with powdery mildew. Plants were sprayed with 200 μg ml^{-1} OGA solution, leaving the lid on the plant tray for 3 h after each treatment.

Powdery mildew disease phenotyping

Ten days after inoculation, a quantitative disease resistance (QDR) score for each plant was measured as described by Meyer *et al.* (2005) and Wang *et al.* (2018), with wild-type plants included in each inoculation batch as a comparison: 0 = no disease phenotype; 1 = few visible conidia; 2 = visible conidia but less than wild type; 3 = conidia equivalent to wild type; and 4 = more conidia than wild type. For lines that consistently scored 1, 2 or 4, additional more quantitative assays were completed, including spore counts and qPCR of fungal to plant gDNA.

Powdery mildew spore counts

The protocol for quantifying fungal spores on each genotype was adopted from Weßling and Panstruga (2012). Leaves infected with *G. cichoracearum* (6 dpi) were harvested, taking 500 mg of leaves per genotype. Water was added (15 ml) and vortexed for 30 s. The spore solution was filtered through Miracloth (Merck) to remove large debris and leaves. The resulting spore solution was pelleted (5 min, 4000 ***g***), removing the supernatant, and resuspended in 50 μl 10% glycerol. Spores were counted in 10 1-mm^2 fields of a Neubauer-improved haemocytometer (Marienfeld, https://www.marienfeld-superior.com) and the results were averaged over at least three slides, with at least three biological replicates per genotype. Spore counts were normalized to the initial weight of the leaves collected.

Quantitative PCR of fungal and plant gDNA

The protocol for quantifying fungal to plant genomic DNA was as described by Weßling and Panstruga (2012). Leaves infected with *G. cichoracearum* (5 dpi) from approximately 40 plants per biological replicate per genotype were harvested and flash-frozen in liquid nitrogen. Genomic DNA was isolated as previously described (Brouwer *et al.*, 2003). Each sample was ground by adding a 1-mm metal ball and the frozen material was agitated in a MM400 mixer mill (Retsch, https://www.retsch.com) for 1 min at 30 Hz. After grinding, 300 μl of lysis buffer [2.5 M LiCl, 50 mM Tris-HCl, 62.5 mM Na_2-ethylenediamine tetraacetic acid (EDTA), and 4.0% Triton X-100, pH 8.0] and 300 μl phenol:chloroform:isoamyl alcohol (25:24:1 v/v) were added and the samples vortexed. Samples were centrifuged (5 min, 16 000 ***g***) and the supernatant was precipitated by two volumes of 100% ethanol, pelleted by centrifugation again, washed in 70% ethanol, air-dried and then resuspended in 50 μl of water. DNA quality and concentration were assessed on a NanoDrop (NanoDro 8000 Spectrophotometer, ThermoFisher Scientific). For Q-PCR, 15-μl samples were prepared using the Brilliant Sybr Green QPCR Reagent Kit (Stratagene, https://go.strategene.org), according to the manufacturer's instructions. Three technical replicates per sample and a primer concentration of 0.4 μM were used. The qPCR program was: denaturation at 95°C for 3 min, 40 repeats of 95°C for 20 s, 61°C for 20 s and 72°C for 15 s. A melting curve analysis was completed from 55°C to 95°C in 0.5°C steps with a 10-s dwell time. The ratio of *G. cichoracearum* to Arabidopsis genomic DNA was calculated using the $\Delta\Delta C_t$ method (Pfaffl, 2001). Primers for Q-PCR are listed in Table S2.

Expression analysis

Total RNA was extracted using the RNeasy plant mini kit (Qiagen), following the manufacturer's instructions. RNA preparations were treated with DNase1 (Qiagen) to remove traces of DNA contamination. RNA (1 μg) was used for reverse transcription with the Transcriptor high-fidelity cDNA synthesis kit (Roche) and oligo dT primers. After synthesis, the cDNA reaction was diluted four times in RNAse-free water, and 2 μl was used for RT-PCR using gene-specific primers (Table S2).

Molecular phylogenetic analysis of the PC-esterase domain by maximum-likelihood method

The evolutionary history was inferred by using the maximum-likelihood method using the JTT matrix-based model (Jones *et al.*, 1992). The tree with the highest log likelihood (-2467.1125) is shown (Figure S5). The initial tree(s) for the heuristic search

was obtained automatically by applying Neighbor-Join and BioNJ algorithms to a matrix of pairwise distances estimated using a JTT model, and then selecting the topology with superior log-likelihood value. The tree is drawn to scale, with branch lengths measured in the number of substitutions per site (next to the branches). The analysis involved 28 amino acid sequences. All positions containing gaps and missing data were eliminated. There were a total of 39 positions in the final data set. Evolutionary analyses were conducted in MEGA 7 (Kumar *et al.*, 2016).

Botrytis susceptibility assays and camalexin quantification

Assays for *Botrytis* susceptibility were completed as previously described (Denby *et al.*, 2004; Kliebenstein *et al.*, 2005). In brief, a total of 20 plants per mutant and a wild-type control (Col-0) were grown in a randomized complete block design for 5 weeks. Plants were sown on soil (Sunshine Mix #1; Sun Gro Horticulture, http://www.sungro.com) under full-spectrum lights using short-day conditions (10 h light). At 5 weeks of age, the first true, mature leaves of each plant were collected and placed on growing flats containing 1% Phytagar. Detached leaves were infected using 4 μl of a half-strength organic grape juice control or a spore suspension containing 10 spores per μl of one of four genotypically diverse isolates (Apple517, B05.10, Supersteak or UKRazz). Infected leaves were incubated for 72 h at room temperature under constant light. Experiments were fully replicated using different growing chambers with 2 weeks between plantings.

Pictures of infected leaves were taken at 72 hpi with a 1-cm reference scale on the flat and leaves were placed in 400 μl of 90% methanol for camalexin extraction. To measure the lesion area, pictures were analyzed using the R package EBIMAGE to isolate the lesion from the leaf and to calculate the lesion area.

Camalexin content was determined as previously described (Corwin *et al.*, 2016a,b). In brief, leaves were ground in methanol, centrifuged to remove precipitate, and 300 μl of supernatant was transferred to a fresh micro-titer plate. A total of 50 μl of extract was sampled and run on an Agilent 1100 series HPLC equipped with a Agilent Lichrocart 250-4 RP18e 5 μm column (Agilent, https://www.agilent.com). The separation of camalexin was accomplished using an acetonitrile and water gradient according to the following program: 5-min gradient from 63% to 69% acetonitrile, 30-s gradient from 69% to 99% acetonitrile, 2 min at 99% acetonitrile and a post-run equilibration of 3.5 min at 63% acetonitrile. The detection of camalexin was achieved with an Agilent fluorescence detector (FLD) with excitation of 318 nm and emission detection at 385 nm. A standard curve using purified camalexin was used to identify and quantitate camalexin from *in vivo* samples.

Statistical analyses

A Student's *t*-test was used to determine the significance of differences found in cell wall biochemistry, as measured in the activity assays, with the levels of significance indicated as: $*P < 0.05$, $**P < 0.01$ and $***P < 0.001$. For differences in spore counts and quantitative gDNA qPCR measurements, the significance was determined with an analysis of variance (ANOVA) test followed by a Tukey's *post-hoc* test.

For *Botrytis* test results, significance testing for the effect of each cell wall mutant was determined separately for lesion area (Table S3) and camalexin content (Table S4) by including all individual alleles in a single general linear model (GLM). *F*-tests were derived from these linear models using the following expression:

$$\begin{aligned} Y_{egrpst} = {} & E_e + I_i + I_i(G_g) + R_r + P_p + S_s + T_t + R:P_{rp} \\ & + T:P_{tp} + I_i(G_g):R_r + I_i(G_g):P_p + I_i(G_g):S_s \\ & + I_i(G_g):T_t + I_i(G_g):R_r:P_p + I_i(G_g):T_t:P_p + \varepsilon_{eigrpst} \end{aligned},$$

where Y is the dependent phenotype (lesion area or camalexin). The main fixed effects are denoted as E, I, G, R, P, S and T, which represent the experimental block, infection status (i.e. uninfected control vs infected), fungal genotype, RWA2-3 allele, PMR5 allele, PMR6 allele and TBR1-1 allele, respectively, with $e = 1,2$; $i = 1,2$; $g = 1...4$; $r = 1,2$; $p = 1,2$; $s = 1,2$; and $t = 1,2$. The fungal genotype was nested within the infection status in order to avoid overestimating the significance of the treatment. All *P* values were derived from a type-II sum of squares and the residual error was assumed to follow a multivariate normal distribution [$\sim N(0,2)$].

DATA AVAILABILITY STATEMENT

All data referred to are included in the article or supplementary materials.

ACKNOWLEDGEMENTS

We thank Gustavo Garcia and Jasmin Chau Tran for technical assistance. We thank Clarice de Azevedo Souza, Nadav Sorek and Trevor Yeats for helpful discussions. We thank Bradley Dotson for *pmr5 tbr1* seed stock. This work was supported by the Energy Biosciences Institute and NSF IOS 1339125 to DK. This work was part of the DOE Joint BioEnergy Institute (http://www.jbei.org) and the DOE Joint Genome Institute (http://www.jgi.org) supported by the US Department of Energy, Office of Science, Office of Biological and Environmental Research, through contract DE-AC02-05CH11231 between Lawrence Berkeley National Laboratory and the US Department of Energy.

CONFLICT OF INTEREST

The authors declare no competing interests.

AUTHOR CONTRIBUTIONS

SS, DK and HS supervised this study. DC, WU, JC, AR, HS, CCC and DB collected the data, and DC and JC performed the data analysis. JV mutagenized *pmr5* and screened for disease suppressor mutants. DC wrote the article with input from the other authors.

SUPPORTING INFORMATION

Additional Supporting Information may be found in the online version of this article.

Figure S1. Cell wall characterization of the *pmr5* mutant in multiple tissues and time points.

Figure S2. Sequentially extracted cell walls of 5-week-old leaves in the *pmr5* mutant.

Figure S3. Chromatography profile of OGAs solution.

Figure S4. PMR5 purification from *E. coli*.

Figure S5. Molecular phylogenetic analysis of previously identified PC-esterase domain members by maximum-likelihood method.

Figure S6. Conservation of catalytic triad in other species.

Figure S7. Expression of *PMR5* in 3-week-old leaves of wild type and *pmr5*.

Figure S8. Powdery mildew disease phenotype in single and double *pmr6* mutants.

Figure S9. Microscopy of the PMR5-GFP protein in three site-directed mutants in the pmr5 mutant background.

Table S1. Cell wall characterization of two cell wall mutant suppressors of powdery mildew disease resistance.

Table S2. List of primers used for genotyping, gene cloning, and quantitative PCR.

Table S3. ANOVA table (type-II tests) for lesion area of *pmr5* and two suppressors of powdery mildew resistance.

Table S4. ANOVA table (type-II tests) for camalexin content of *pmr5* and two suppressors of powdery mildew resistance.

REFERENCES

Adam, L. and Somerville, S.C. (1996) Genetic characterization of five powdery mildew disease resistance loci in Arabidopsis thaliana. *Plant J.* **9**(3), 341–356.

Anantharaman, V. and Aravind, L. (2010) Novel eukaryotic enzymes modifying cell-surface biopolymers. *Biol. Direct*, **5**, 1.

Arming, S., Wipfler, D., Mayr, J., Merling, A., Vilas, U., Schauer, R., Schwartz-Albiez, R. and Vlasak, R. (2011) The human Cas1 protein: a Sialic Acid-Specific O-Acetyltransferase? *Glycobiology*, **21**(5), 553–564.

Bellincampi, D., Cervone, F. and Lionetti, V. (2014) Plant cell wall dynamics and wall-related susceptibility in plant–pathogen interactions. *Front. Plant Sci.* **5**, 228. https://doi.org/10.3389/fpls.2014.00228.

Bellincampi, D., Dipierro, N., Salvi, G., Cervone, F. and De Lorenzo, G. (2000) Extracellular H2O2 induced by oligogalacturonides is not involved in the inhibition of the auxin-regulated rolB gene expression in tobacco leaf explants. *Plant Physiol.* **122**(4), 1379–1386.

Bischoff, V., Nita, S., Neumetzler, L., Schindelasch, D., Urbain, A., Eshed, R., Persson, S., Delmer, D. and Scheible, W.-R. (2010) TRICHOME BIREFRINGENCE and its homolog AT5G01360 encode novel plant-specific DUF231 proteins required for cellulose biosynthesis in Arabidopsis. *Plant Physiol.* **153**(2), 590–602.

Brouwer, M., Lievens, B., Van Hemelrijck, W., Van den Ackerveken, G., Cammue, B.P. and Thomma, B.P. (2003) Quantification of disease progression of several microbial pathogens on Arabidopsis thaliana using real-time fluorescence PCR. *FEMS Microbiol. Lett.* **228**(2), 241–248.

Brummell, D.A. (2006) Cell wall disassembly in ripening fruit. *Funct. Plant Biol.* **33**(2), 103–119.

Brutus, A., Sicilia, F., Macone, A., Cervone, F. and De Lorenzo, G. (2010) A domain swap approach reveals a role of the plant wall-associated Kinase 1 (WAK1) as a receptor of oligogalacturonides. *Proc. Natl Acad. Sci. USA*, **107**(20), 9452–9457.

Caffall, K.H. and Mohnen, D. (2009) The structure, function, and biosynthesis of plant cell wall pectic polysaccharides. *Carbohyd. Res.* **344**(14), 1879–1900.

Clough, S.J. and Bent, A.F. (1998) Floral dip: a simplified method for Agrobacterium-mediated transformation of Arabidopsis thaliana. *Plant J.* **16**(6), 735–743.

Corwin, J.A., Copeland, D., Feusier, J., Subedy, A., Eshbaugh, R., Palmer, C., Maloof, J. and Kliebenstein, D.J. (2016a) The quantitative basis of the Arabidopsis innate immune system to endemic pathogens depends on pathogen genetics. *PLoS Genet.* **12**(2), e1005789.

Corwin, J.A., Subedy, A., Eshbaugh, R. and Kliebenstein, D.J. (2016b) Expansive phenotypic landscape of botrytis cinerea shows differential contribution of genetic diversity and plasticity. *Mol. Plant Microbe Interact.* **29**(4), 287–298.

Cosgrove, D.J. (2005) Growth of the plant cell wall. *Nat. Rev. Mol. Cell Biol.* **6**(11), 850–861.

Curtis, M.D. and Grossniklaus, U. (2003) A gateway cloning vector set for high-throughput functional analysis of genes in planta. *Plant Physiol.* **133**(2), 462–469.

Denby, K.J., Kumar, P. and Kliebenstein, D.J. (2004) Identification of Botrytis Cinerea susceptibility loci in Arabidopsis Thaliana. *Plant J.* **38**(3), 473–486.

Ferrari, S., Galletti, R., Denoux, C., De Lorenzo, G., Ausubel, F.M. and Dewdney, J. (2007) Resistance to Botrytis Cinerea induced in Arabidopsis by elicitors is independent of salicylic acid, ethylene, or jasmonate signaling but requires PHYTOALEXIN DEFICIENT3. *Plant Physiol.* **144**(1), 367–379.

Ferrari, S., Galletti, R., Pontiggia, D., Manfredini, C., Lionetti, V., Bellincampi, D., Cervone, F. and De Lorenzo, G. (2008) Transgenic expression of a fungal endo-polygalacturonase increases plant resistance to pathogens and reduces auxin sensitivity. *Plant Physiol.* **146**(2), 669–681.

Ferrari, S., Savatin, D.V., Sicilia, F., Gramegna, G., Cervone, F. and De Lorenzo, G. (2013) Oligogalacturonides: plant damage-associated molecular patterns and regulators of growth and development. *Front. Plant Sci.* **4**, 49. https://doi.org/10.3389/fpls.2013.00049.

Gille, S., Cheng, K., Skinner, M.E., Liepman, A.H., Wilkerson, C.G. and Pauly, M. (2011a) Deep sequencing of Voodoo Lily (Amorphophallus Konjac): an approach to identify relevant genes involved in the synthesis of the Hemicellulose Glucomannan. *Planta*, **234**(3), 515–526.

Gille, S., de Souza, A., Xiong, G., Benz, M., Cheng, K., Schultink, A., Reca, I.-B. and Pauly, M. (2011b) O-Acetylation of Arabidopsis Hemicellulose Xyloglucan requires AXY4 or AXY4L, proteins with a TBL and DUF231 domain. *Plant Cell*, **23**(11), 4041–4053.

Glawe, D.A. (2008) The powdery mildews: a review of the World's most familiar (yet Poorly Known) plant pathogens. *Annu. Rev. Phytopathol.* **46**, 27–51.

Glazebrook, J. (2005) Contrasting mechanisms of defense against biotrophic and necrotrophic pathogens. *Annu. Rev. Phytopathol.* **43**, 205–227.

Hamann, T. (2012) Plant cell wall integrity maintenance as an essential component of biotic stress response mechanisms. *Front. Plant Sci.* **3**, 77.

Harholt, J., Jensen, J.K., Sørensen, S.O., Orfila, C., Pauly, M. and Scheller, H.V. (2006) ARABINAN DEFICIENT 1 Is a putative arabinosyltransferase involved in biosynthesis of pectic arabinan in Arabidopsis. *Plant Physiol.* **140**(1), 49–58.

Harholt, J., Suttangkakul, A. and Scheller, H.V. (2010) Biosynthesis of pectin. *Plant Physiol.* **153**(2), 384–395.

Hotchkiss, A.T. Jr and Hicks, K.B. (1990) Analysis of oligogalacturonic acids with 50 or fewer residues by high-performance anion-exchange chromatography and pulsed amperometric detection. *Anal. Biochem.* **184**(2), 200–206.

Janbon, G., Himmelreich, U., Moyrand, F., Improvisi, L. and Dromer, F. (2001) Cas1p is a membrane protein necessary for the O-Acetylation of the Cryptococcus Neoformans Capsular Polysaccharide. *Mol. Microbiol.* **42**(2), 453–467.

Jones, D.T., Taylor, W.R. and Thornton, J.M. (1992) The rapid generation of mutation data matrices from protein sequences. *Comput. Appl. Biosci.* **8**(3), 275–282.

Kämper, J., Kahmann, R., Bölker, M. *et al.* (2006) Insights from the genome of the biotrophic fungal plant pathogen Ustilago Maydis. *Nature*, **444**(7115), 97–101.

Keegstra, K. (2010) Plant cell walls. *Plant Physiol.* **154**(2), 483–486.

Kliebenstein, D.J., Rowe, H.C. and Denby, K.J. (2005) Secondary metabolites influence Arabidopsis/Botrytis interactions: variation in host production and pathogen sensitivity. *Plant J.* **44**(1), 25–36.

Kohorn, B.D. and Kohorn, S.L. (2012) The cell wall-associated Kinases, WAKs, as pectin receptors. *Front. Plant Sci.* **3**, 88. https://doi.org/10.3389/fpls.2012.00088.

Koncz, C. and Schell, J. (1986) The promoter of TL-DNA gene 5controls the tissue-specific expression of chimaeric genes carried by a novel type of Agrobacterium binary vector. *Mol. Gen. Genet.* **204**, 383. https://doi.org/10.1007/BF00331014.

Kumar, S., Stecher, G. and Tamura, K. (2016) MEGA7: molecular evolutionary genetics analysis version 7.0 for bigger datasets. *Mol. Biol. Evol.* **33**(7), 1870–1874.

Lee, C., O'Neill, M.A., Tsumuraya, Y., Darvill, A.G. and Ye, Z.-H. (2007) The irregular xylem9 mutant is deficient in xylan xylosyltransferase activity. *Plant and Cell Physiol.* **48**(11), 1624–1634. https://doi.org/10.1093/pcp/pcm135.

Liners, F., Thibault, J.-F. and Van Cutsem, P. (1992) Influence of the degree of polymerization of Oligogalacturonates and of Esterification pattern of

pectin on their recognition by monoclonal antibodies. *Plant Physiol.* **99** (3), 1099–1104.

Lionetti, V., Cervone, F. and Bellincampi, D. (2012) Methyl esterification of pectin plays a role during plant-pathogen interactions and affects plant resistance to diseases. *J. Plant Physiol.* **169**(16), 1623–1630.

Lionetti, V., Raiola, A., Cervone, F. and Bellincampi, D. (2014) Transgenic expression of pectin methylesterase inhibitors limits tobamovirus spread in tobacco and Arabidopsis. *Mol. Plant Pathol.* **15**(3), 265–274.

Lionetti, V., Fabri, E., De Caroli, M., Hansen, A.R., Willats, W.G.T., Piro, G. and Bellincampi, D. (2017) Three pectin methylesterase inhibitors protect cell wall integrity for Arabidopsis immunity to Botrytis. *Plant Physiol.* **173** (3), 1844–1863.

Lukowitz, W., Meyer, U. and Jürgens, G. (1996) Cytokinesis in the Arabidopsis embryo involves the syntaxin-related KNOLLE gene product. *Cell*, **84**, 61–71.

Manabe, Y., Nafisi, M., Verhertbruggen, Y. *et al.* (2011) Loss-of-function mutation of REDUCED WALL ACETYLATION2 in Arabidopsis leads to reduced cell wall acetylation and increased resistance to Botrytis Cinerea. *Plant Physiol.* **155**(3), 1068–1078.

Manabe, Y., Verhertbruggen, Y., Gille, S. *et al.* (2013) RWA proteins play vital and distinct roles in cell wall O-Acetylation in Arabidopsis Thaliana. *Plant Physiol.* **163**, 1107–1117.

Meyer, D., Lauber, E., Roby, D., Arlat, M. and Kroj, T. (2005) Optimization of pathogenicity assays to study the Arabidopsis Thaliana-Xanthomonas Campestris Pv. Campestris Pathosystem. *Mol. Plant Pathol.* **6**(3), 327–333.

Mohnen, D. (2008) Pectin structure and biosynthesis. *Curr. Opin. Plant Biol.* **11**(3), 266–277.

Nafisi, M., Stranne, M., Fimognari, L. *et al.* (2015) Acetylation of cell wall is required for structural integrity of the leaf surface and exerts a global impact on plant stress responses. *Front. Plant Sci.* **6**, 550.

O'Connell, R.J., Thon, M.R., Hacquard, S. *et al.* (2012) Lifestyle transitions in plant pathogenic Colletotrichum Fungi deciphered by genome and transcriptome analyses. *Nat. Genet.* **44**(9), 1060–1065.

Osorio, S., Bombarely, A., Giavalisco, P., Usadel, B., Stephens, C., Aragüez, I., Medina-Escobar, N., Botella, M.A., Fernie, A.R. and Valpuesta, V. (2011) Demethylation of Oligogalacturonides by FaPE1 in the fruits of the wild strawberry Fragaria Vesca triggers metabolic and transcriptional changes associated with defence and development of the fruit. *J. Exp. Bot.* **62**(8), 2855–2873.

Pfaffl, M.W. (2001) A new mathematical model for relative quantification in real-time RT-PCR. *Nucleic Acids Res.* **29**(9), e45.

Randoux, B., Renard-Merlier, D., Mulard, G., Rossard, S., Duyme, F., Sanssené, J., Courtois, J., Durand, R. and Reignault, P. (2010) Distinct defenses induced in wheat against powdery mildew by acetylated and nonacetylated oligogalacturonides. *Phytopathology*, **100**(12), 1352–1363.

Rennie, E.A., Hansen, S.F., Baidoo, E.E.K., Hadi, M.Z., Keasling, J.D. and Scheller, H.V. (2012) Three members of the Arabidopsis glycosyltransferase family 8 are Xylan Glucuronosyltransferases1[W][OA]. *Plant Physiol.* **159**(4), 1408–1417.

Schultink, A., Naylor, D., Dama, M. and Pauly, M. (2015) The role of the plant-specific ALTERED XYLOGLUCAN9 protein in Arabidopsis cell wall Polysaccharide O-Acetylation. *Plant Physiol.* **167**(4), 1271–1283.

Schulze-Lefert, P. and Vogel, J. (2000) Closing the ranks to attack by powdery mildew. *Trends Plant Sci.* **5**(8), 343–348.

Selig, M.J., Vinzant, T.B., Himmel, M.E. and Decker, S.R. (2009) The effect of lignin removal by alkaline peroxide pretreatment on the susceptibility of corn stover to purified cellulolytic and xylanolytic enzymes. *Appl. Biochem. Biotechnol.* **155**(1–3), 397–406.

Somerville, C., Bauer, S., Brininstool, G. *et al.* (2004) Toward a systems approach to understanding plant cell walls. *Science*, **306**(5705), 2206–2211.

Stranne, M., Ren, Y., Fimognari, L. *et al.* (2018) TBL10 is required for O-Acetylation of pectic Rhamnogalacturonan-I in Arabidopsis Thaliana. *Plant J.* **96**(4), 772–785.

Underwood, W. (2012) The plant cell wall: a dynamic barrier against pathogen invasion. *Front. Plant Sci.* **3**, 85. https://doi.org/10.3389/fpls.2012.00085.

Urbanowicz, B.R., Peña, M.J., Moniz, H.A., Moremen, K.W. and York, W.S. (2014) Two Arabidopsis proteins synthesize acetylated Xylan in vitro. *Plant J.* **80**(2), 197–206.

Vogel, J. and Somerville, S. (2000) Isolation and characterization of powdery mildew-resistant Arabidopsis mutants. *Proc. Natl Acad. Sci. USA*, **97**(4), 1897–1902.

Vogel, J.P., Raab, T.K., Schiff, C. and Somerville, S.C. (2002) PMR6, a Pectate Lyase-Like gene required for powdery mildew susceptibility in Arabidopsis. *Plant Cell*, **14**(9), 2095–2106.

Vogel, J.P., Raab, T.K., Somerville, C.R. and Somerville, S.C. (2004) Mutations in PMR5 result in powdery mildew resistance and altered cell wall composition. *Plant J.* **40**(6), 968–978.

Volpi, C., Janni, M., Lionetti, V., Bellincampi, D., Favaron, F. and D'Ovidio, R. (2011) The ectopic expression of a pectin methyl esterase inhibitor increases pectin methyl esterification and limits fungal diseases in wheat. *Mol. Plant Microbe Interact.* **24**(9), 1012–1019.

Wang, M., Roux, F., Bartoli, C., Huard-Chauveau, C., Meyer, C., Lee, H., Roby, D., McPeek, M.S. and Bergelson, J. (2018) Two-way mixed-effects methods for joint association analysis using both host and pathogen genomes. *Proc. Natl Acad. Sci. USA*, **115**(24), E5440–E5449.

Weßling, R. and Panstruga, R. (2012) Rapid quantification of plant-powdery mildew interactions by qPCR and conidiospore counts. *Plant Methods*, **8** (1), 35. https://doi.org/10.1186/1746-4811-8-35.

Xin, Z., Mandaokar, A., Chen, J., Last, R.L. and Browse, J. (2007) Arabidopsis ESK1 encodes a novel regulator of freezing tolerance. *Plant J.* **49**(5), 786–799.

Yin, L., Verhertbruggen, Y., Oikawa, A. *et al.* (2011) The cooperative activities of CSLD2, CSLD3, and CSLD5 are required for normal Arabidopsis development. *Mol. Plant*, **4**(6), 1024–1037.

Yuan, Y., Teng, Q., Zhong, R. and Ye, Z.-H. (2013) The Arabidopsis DUF231 domain-containing protein ESK1 mediates 2-O- and 3-O-Acetylation of Xylosyl residues in Xylan. *Plant Cell Physiol.* **54**(7), 1186–1199.

Yuan, Y., Teng, Q., Zhong, R. and Ye, Z.-H. (2016) TBL3 and TBL31, two Arabidopsis DUF231 domain proteins, are required for 3-O-Monoacetylation of Xylan. *Plant Cell Physiol.* **57**(1), 35–45.

Zhu, X.F., Sun, Y., Zhang, B.C., Mansoori, N., Wan, J.X., Liu, Y., Wang, Z.W., Shi, Y.Z., Zhou, Y.H. and Zheng, S.J. (2014) TRICHOME BIREFRINGENCE-LIKE27 affects aluminum sensitivity by modulating the O-Acetylation of Xyloglucan and Aluminum-binding capacity in Arabidopsis. *Plant Physiol.* **166**(1), 181–189.